Science Signaling
AAAS

www.sciencesignaling.org/cgi/content/full/10/494/eaak9702/DC1

Supplementary Materials for

Blockade of surface-bound TGF-β on regulatory T cells abrogates suppression of effector T cell function in the tumor microenvironment

Sadna Budhu, David A. Schaer, Yongbiao Li, Ricardo Toledo-Crow, Katherine Panageas, Xia Yang, Hong Zhong, Alan N. Houghton, Samuel C. Silverstein, Taha Merghoub,* Jedd D. Wolchok*

*Corresponding author. Email: merghout@mskcc.org (T.M.); wolchokj@mskcc.org (J.D.W.)

Published 29 August 2017, *Sci. Signal.* **10**, eaak9702 (2017)
DOI: 10.1126/scisignal.aak9702

The PDF file includes:

Other Supplementary Material for this manuscript includes the following:
(available at www.sciencesignaling.org/cgi/content/full/10/494/eaak9702/DC1)

Summary of statistical analyses

Fig. 2B. 24 hours

Kruskal-Wallis test: $P < 0.007$

Pairwise comparisons using Wilcoxon rank sum test with post hoc Bonferroni correction:

Cultured B16 vs. 3D gels: not significant

Cultured B16 vs. 2D culture: $P = 0.018$

3D gels vs 2D culture: $P = 0.018$

Fig. 2B. 48 hours

Kruskal-Wallis test: $P < 0.0008$

Pairwise comparisons using Wilcoxon rank sum test with post hoc Bonferroni correction:

Cultured B16 vs. 3D gels: $P = 0.012$

Cultured B16 vs. 2D culture: $P = 0.018$

3D gels vs. 2D culture: $P = 0.018$

Fig. 2C. 24 hours

Kruskal-Wallis test: $P < 0.007$

Pairwise comparisons using Wilcoxon rank sum test with post hoc Bonferroni correction:

Cultured B16 vs. 3D gels: not significant

Cultured B16 vs. 2D culture: $P = 0.018$

3D gels vs. 2D culture: $P = 0.018$

Fig. 2C. 48 hours

Kruskal-Wallis test: $P < 0.0008$

Pairwise comparisons using Wilcoxon rank sum test with post hoc Bonferroni correction:

Cultured B16 vs. 3D gels: $P = 0.012$

Cultured B16 vs. 2D culture: $P = 0.018$

3D gels vs. 2D culture: $P = 0.018$

Fig. 2D.

Wilcoxon rank sum test: not significant

Fig. 3C. 24 hours

Kruskal-Wallis test: $P < 0.003$

Pairwise comparisons using Wilcoxon rank sum test with post hoc Bonferroni correction:

Nondepleted vs. T_{reg}-depleted: $P = 0.012$

Nondepleted vs. cultured B16: $P = 0.018$

T_{reg}-depleted vs. cultured B16: not significant

Fig. 3C. 48 hours

Kruskal-Wallis test: $P < 0.003$

Pairwise comparisons using Wilcoxon rank sum test with post hoc Bonferroni correction:

Nondepleted vs. T_{reg}-depleted: $P = 0.015$

Nondepleted vs. cultured B16: $P = 0.015$

T_{reg}-depleted vs. cultured B16: not significant

Fig. 3D. 24 hours
Kruskal-Wallis test: $P < 0.003$
Pairwise comparisons using Wilcoxon rank sum test with post hoc Bonferroni correction:
Nondepleted vs. T_{reg}-depleted*:* $P = 0.012$
Nondepleted vs. cultured B16: $P = 0.012$
T_{reg}-depleted vs. cultured B16: not significant

Fig. 3D. 48 hours
Kruskal-Wallis test: $P < 0.002$
Pairwise comparisons using Wilcoxon rank sum test with post hoc Bonferroni correction:
Nondepleted vs. T_{reg}-depleted: $P = 0.012$
Nondepleted vs. cultured B16: $P = 0.012$
T_{reg}-depleted vs. cultured B16: $P = 0.012$

Fig. 4A. Tumor
Kruskal-Wallis test: $P < 0.011$

The only pairwise comparison was between the no antibody condition and the anti-TGF-β antibody condition: $P = 0.004$ by Wilcoxon rank sum test. .

Fig. 4A. Cultured cells
Kruskal-Wallis test: not significant

The only pairwise comparison was between the no antibody condition and the anti-TGF-β antibody condition: not significant by Wilcoxon rank sum test.

Fig. 4B. Tumor
Kruskal-Wallis test: $P < 0.016$

The only pairwise comparison was between the no antibody condition and the anti-TGF-β antibody condition: $P = 0.004$ by Wilcoxon rank sum test.

Fig. 4B. Cultured cells
Kruskal-Wallis test: not significant

The only pairwise comparison was between the no antibody condition and the anti-TGF-β antibody condition: $P = 0.34$ by Wilcoxon rank sum test.

Fig. 6, B and C
A generalized estimating equations model with log link was fit to the data in Figs. 5B and 6C accounting for the repeated time measurements.

Comparison of curves in Fig. 6B:
T_{reg} depleted + OT-1 group compared with T_{regs} depleted + OT-1 + T_{regs}: not significant
anti–TGF-β compared with T_{reg}-depleted + OT-1 + T_{regs}: not significant

Comparison of curves in Fig. 6C:
B16-OVA + OT-1+ T_{regs} vs. B16-OVA + OT-1: $P = 0.06$
B16-OVA + OT-1+ T_{regs} vs. B16-OVA + OT-1 + T_{regs} + anti–TGF-β: $P = 0.08$

Comparison of data in Fig. 6 at 72 hours only
Fig. 6B
Comparison of three groups (OT-1; OT-1 + T_{regs}; OT-1 + T_{regs} + anti–TGF-β) by Kruskal-Wallis test: $P = 0.005$. Because there was an overall difference, group-wise comparisons were assessed using Wilcoxon Mann-Whitney:
OT-1 vs. OT-1 + T_{regs}: $P = 0.015$
OT-1 + T_{regs} vs. OT-1 + T_{regs} + anti–TGF-β: $P = 0.03$
OT-1 vs. OT-1 + T_{regs} + anti–TGF-β: $P = 0.94$

Fig. 6C
Comparison of three groups (OT-1; OT-1 + T_{regs}; OT-1 + T_{regs} + anti–TGF-β) by Kruskal-Wallis test: $P = 0.02$. Because there was an overall difference, group-wise comparisons were assessed using Wilcoxon Mann-Whitney:
OT-1 vs. OT-1+T_{regs}: $P = 0.06$
OT-1 + T_{regs} vs. OT-1+T_{regs} + anti–TGF-β: $P = 0.06$
OT-1 vs. OT-1 + T_{regs}+ anti–TGF-β: $P = 1.41$

Fig. 6D
Granzyme B MFI by Kruskal-Wallis across four groups: $P = 0.05$
PD1 MFI by Kruskal-Wallis across four groups: $P = 0.06$

Granzyme B MFI by Wilcoxon rank sum test for cultured B16 vs. cultured B16 + T_{reg}: $P = 0.13$
PD1 MFI by Wilcoxon rank sum test for cultured B16 vs. cultured B16 +T_{reg}: $P = 0.05$

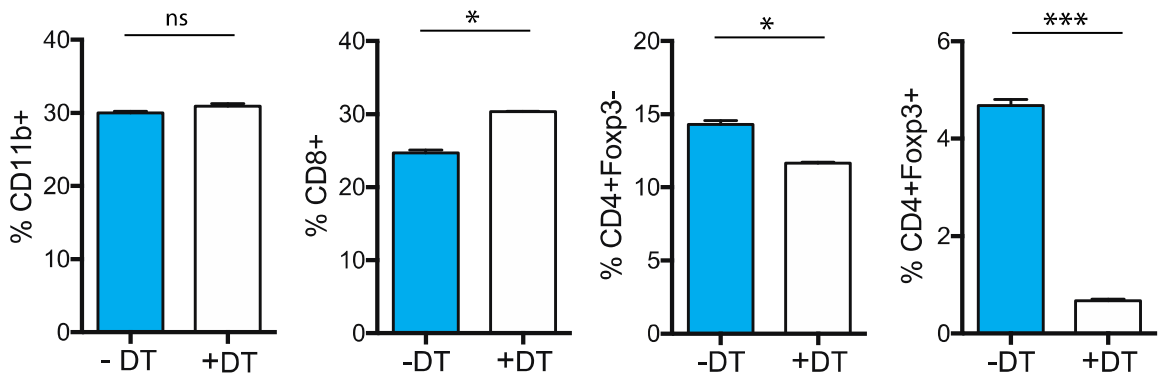

Fig. S1. Analysis of immune cell infiltrates in tumors from DT-treated Foxp3-DTR mice. B16-OVA tumor–bearing Foxp3-DTR mice were treated with DT to deplete T_{regs} 2 days before tumor excision. The immune cell composition of the tumors was then analyzed by flow cytometry with anti-CD45, anti-CD11b, anti-CD8, anti-CD4, and anti-Foxp3 antibodies after the cells were purified by Percoll gradient. The frequencies of the indicated cell types are reported as mean percentages ± SEM of live (viability dye–negative) $CD45^+$ cells in triplicate samples from pooled tumors (n = 5 mice per group) and are from one experiment that is representative of two independent experiments. $*P \leq 0.05$, $***P \leq 0.005$.

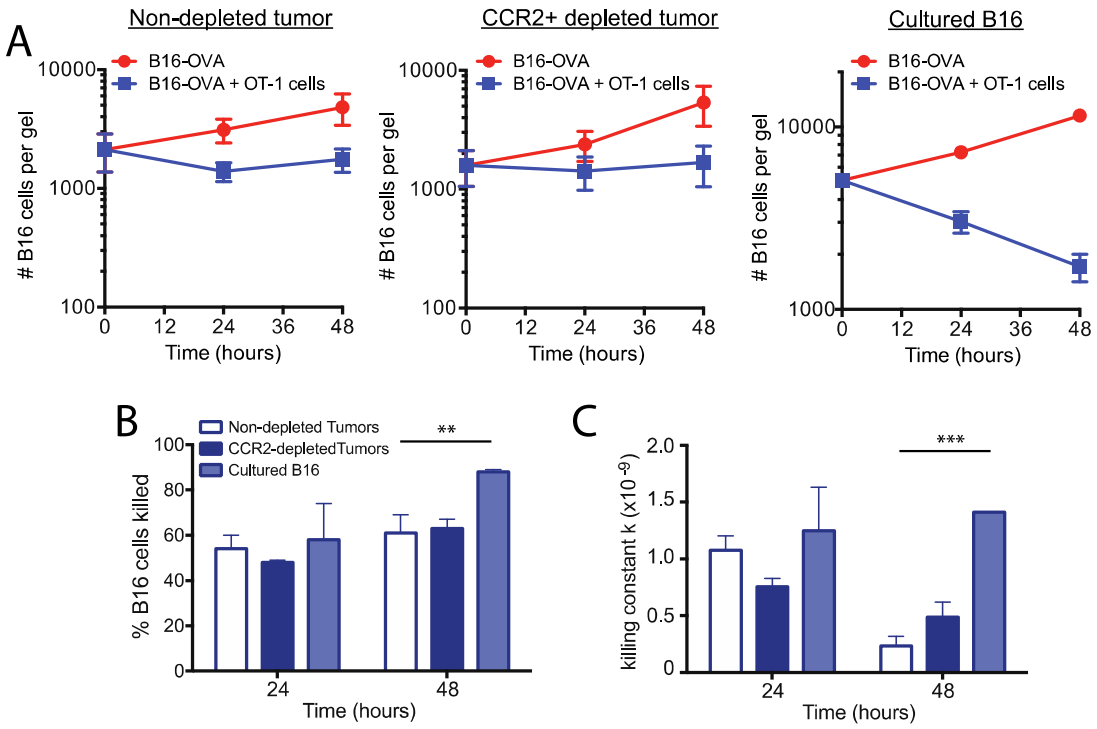

Fig. S2. In vivo depletion of CCR2$^+$ cells in CCR2-DTR mice has no effect on the suppression of CD8$^+$ T cell–mediated killing by the tumor microenvironment. (**A** to **C**) Tumor-bearing CCR2-DTR mice were treated with DT to deplete CCR2-expressing cells 2 days before tumor excision (as described in Materials and Methods) and the tumors were excised and dissociated on day 11. Dissociated CCR2-depleted tumors, nondepleted tumors, and cultured B16-OVA cells were co-embedded in collagen-fibrin gels with in vitro–activated OT-1 cells at a ratio of 50:1 effector cells to target cells. (A) At the indicated times, the gels were dissolved and the numbers of remaining B16 cells were measured with a clonogenic assay. (B) The percentages of B16 cells that were killed at the indicated times were determined. (C) Average values of k for each condition. Data in (A) to (C) are means ± SEM of two experiments each performed in duplicate. $^{**}P \leq 0.01$, $^{***}P \leq 0.005$.

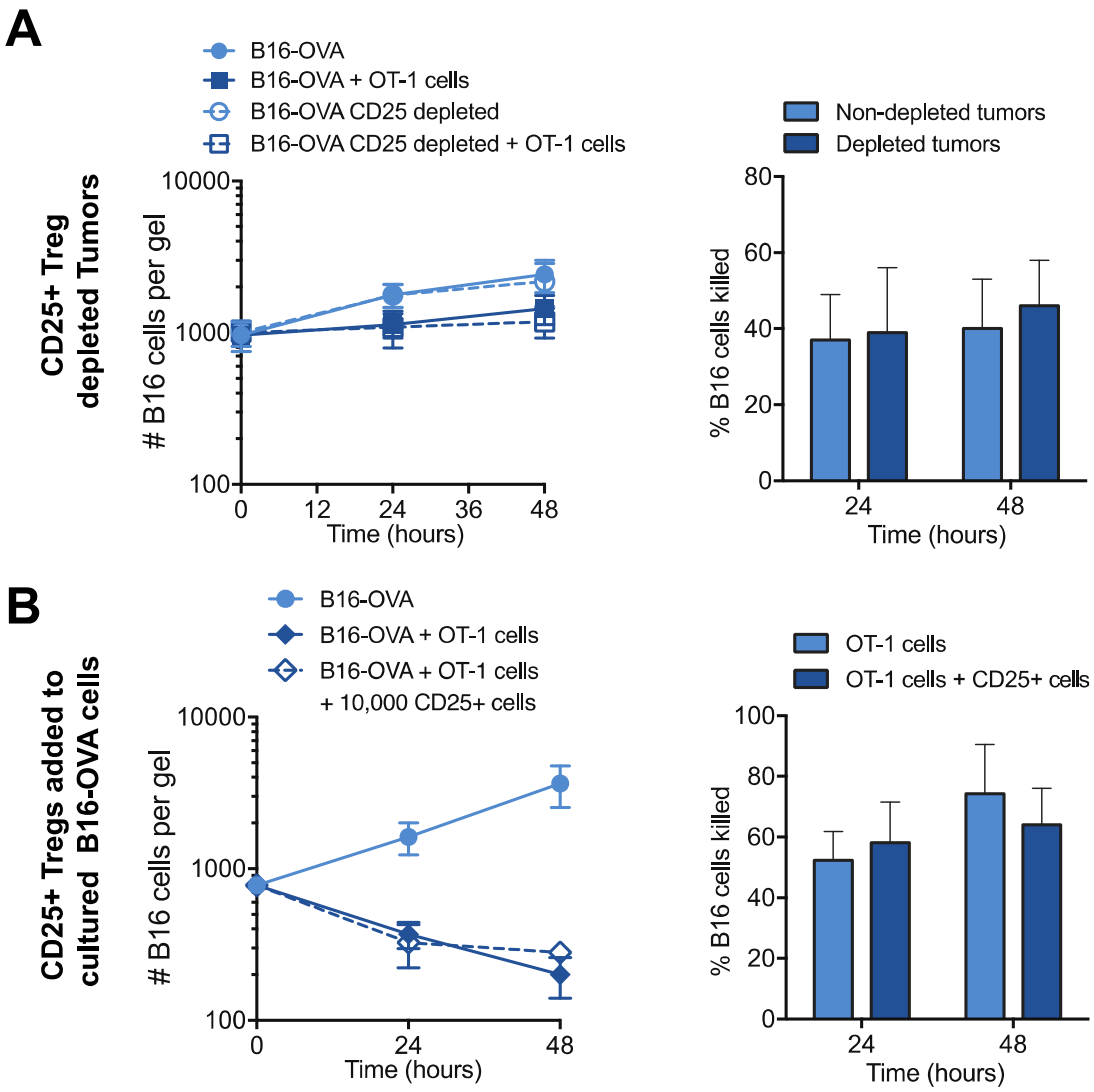

Fig. S3. Depleting T_{regs} ex vivo with anti-CD25 MicroBeads has no effect on the immunosuppression of $CD8^+$ T cells. (**A** and **B**) B16-OVA tumors were excised and dissociated as described in Fig. 1. T_{regs} were purified from the dissociated tumors using the $CD4^+CD25^+$ magnetic bead T_{reg} isolation kit as described in Materials and Methods. CD25-depleted tumors or cultured B16-OVA cells were co-embedded in collagen-fibrin gels with in vitro–activated OT-1 cells at a 50:1 effector to target ratio with or without 10,000 purified $CD4^+CD25^+$ cells. At the indicated times, the gels were dissolved and the numbers of remaining B16 cells were measured using a clonogenic assay. (A) Killing of B16-OVA tumors depleted of $CD4^+CD25^+$ cells. (B) Killing of cultured B16-OVA in the presence of $CD4^+CD25^+$ cells. Data represent the numbers of viable B16 cells and the average percentages of B16 cells killed ± SEM of three experiments each performed in duplicate.

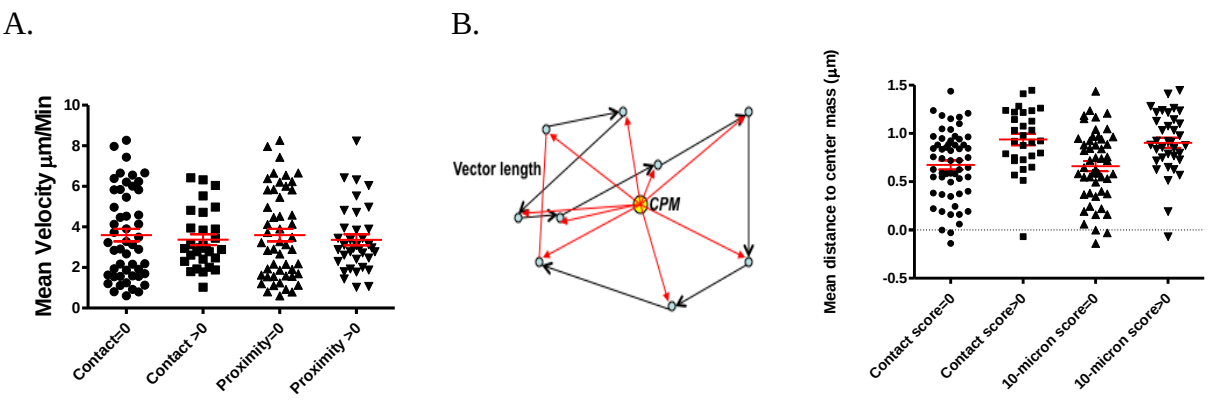

Fig. S4. T_{regs} cause minor alterations to the mobility of $CD8^+$ T cells in the tumor. (**A**) Mean velocity of Pmel-1 T cells that displayed interactions with T_{regs} (Contact > 0 or Proximity within 10 microns >0) compared to Pmel-1 T cells that had no interactions (Contact or proximity = 0). (**B**) Left: Area of movement or mean distance from the center of mass were measured as described previously *(10)* by taking an Average X,Y,Z location for all time points (central point) and then measuring the vector distance from each time point to the central point for each Pmel-1 T cell. Right: Comparison of the mean distance to the center of mass is shown for Pmel-1 T cells with and without interactions with T_{regs}. Pmel-1 T cells that had interactions with T_{regs} displayed an increased area of movement compared to those that did not. $P = 0.0021$ when comparing the contact = 0 condition to the contact > 0 condition; $P = 0.0013$ when comparing the 10 micron = 0 group to the 10 micron > 0 group.

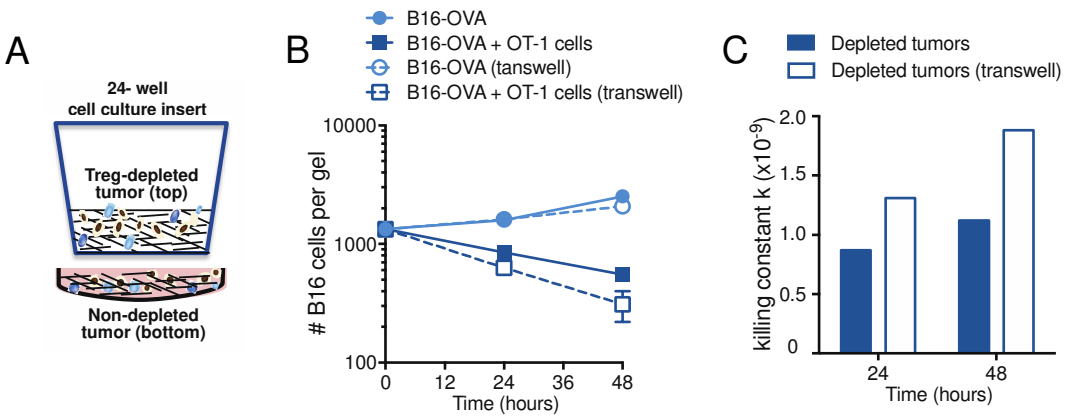

Fig. S5. Suppression of CD8$^+$ T cells by T_{regs} is contact- or proximity-dependent. (**A** to **C**) Mice were treated with DT to deplete T_{regs} 2 days before excision, after which the tumors were excised and dissociated. (A) Dissociated depleted tumors were co-embedded in collagen-fibrin gels with in vitro–activated OT-1 cells at a 50:1 effector to target ratio in the upper chamber of 24-well cell culture inserts and nondepleted tumors were embedded in collagen-fibrin gels in the bottom of the 24-well plate as described in Materials and Methods. (B) At the indicated times, the gels were dissolved and the numbers of remaining B16 cells in the gels were measured using a clonogenic assay. Data represent the number of viable B16 cells ± SEM of duplicate samples from a representative experiment. (C) The value of *k* was calculated using data obtained in (B). A total of two experiments were performed in duplicate with identical results.

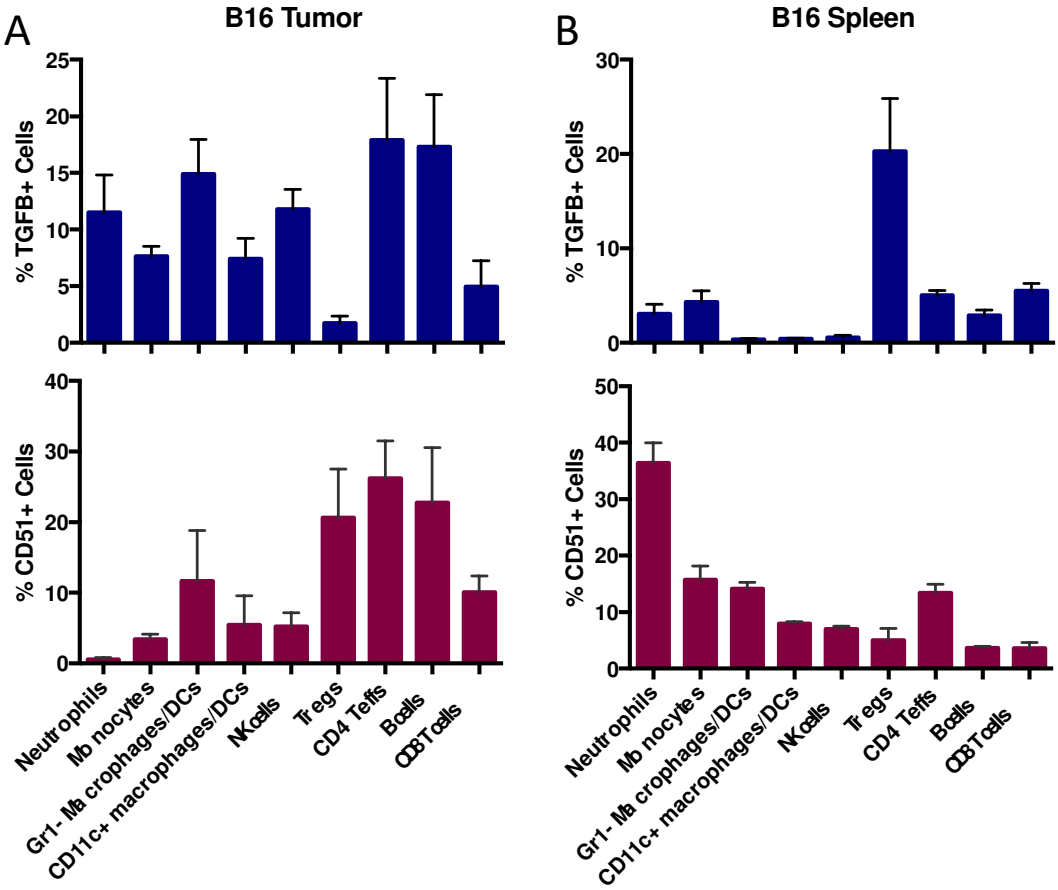

Fig. S6. Expression of TGF-β and CD51 (α_V integrin) in immune cell subsets from the tumors and spleens of B16 tumor–bearing mice. (**A** and **B**) Tumors (A) and spleens (B) were excised from mice 10 days after B16 tumor inoculation and were dissociated into single-cell suspensions. The immune cell composition and their cell surface expression of TGF-β and CD51 were analyzed by flow cytometry using fluorophore-conjugated anti-CD45, anti-Gr1 (for neutrophils, monocytes, and macrophages), anti-CD11c (for macrophages and DCs), anti-NK1.1 (for NK cells), anti-CD4, anti-Foxp3 (for T_{regs}), anti-CD19 (for B cells), anti-CD8, anti-CD51, and anti-TGF-β (clone 1D11) antibodies. The amount of TGF-β protein in the indicated immune cell subsets was examined after the cells were fixed and permeabilized following surface staining. Each cell population was sub-gated from live (viability dye–negative) $CD45^+$ cells and plotted as the percentage of $TGF\beta^+$ or $CD51^+$ cells ± SEM of five mice per group.

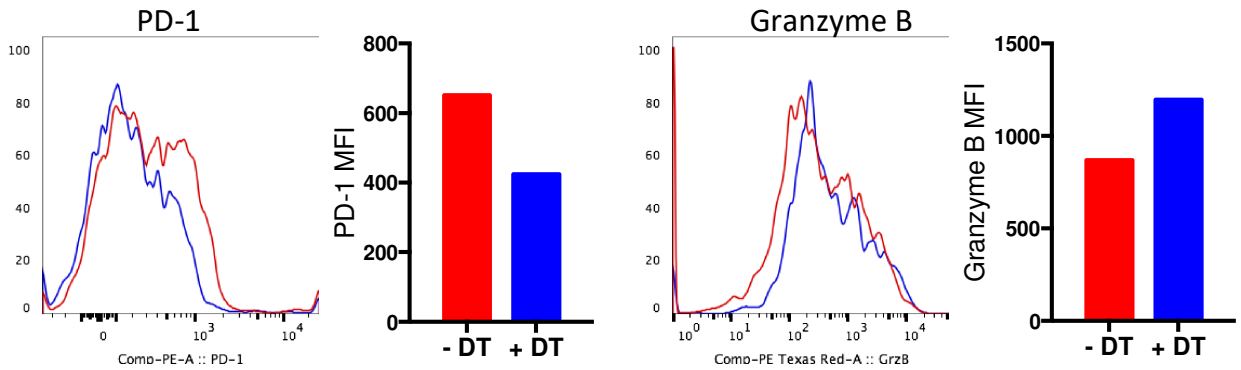

Fig. S7. Effect of DT on the expression of PD-1 and granzyme B on the surface of endogenous CD8$^+$ T cells. Tumor-bearing Foxp3-DTR mice were treated with DT to deplete T_{regs} 2 days before tumor excision. The immune cells and their activation status were analyzed by flow cytometry using fluorophore-conjugated anti-CD45, anti-CD8, anti-PD-1, and anti–granzyme B antibodies after the cells were purified using a percoll gradient. Each bar graph beside the histograms shows the mean fluorescence intensity (MFI) for each protein. Data depicted are representative graphs and the MFIs of pooled tumors from five mice per group.

Movie S1. CFP-Pmel T cells are found in regions highly infiltrated by T_{regs}. Foxp3-GFP mice were subcutaneously injected with YFP-B16 tumor cells in matrigel on the left flank. Three days later, naïve $CD8^+$ CFP-Pmel cells were injected into the mice through the tail vein. Between 4 and 10 days after transfer, the mice were anesthetized and imaged by intravital microscopy as described in Materials and Methods and Fig 5. Time-lapse mages were analyzed for the interactions of $CD8^+$ CFP-Pmel T cells (cyan) with T_{regs} (red), which were analyzed as described in Materials and Methods.

Movie S2. CFP-Pmel T cells are found within proximity to or make contact with T_{regs}. Higher magnification of the time-lapse image of $CD8^+$ CFP-Pmel T cells (cyan) interacting with T_{regs} (red) from the experiment described in Fig. 5 and shown in movie S1.